2

3

DNA methylation marks inter-nucleosome linker

regions throughout the human genome

Benjamin P. Berman^{1,2,3,#}, Yaping Liu^{1,4}, Theresa K. Kelly^{1,2,*} 4 5 6 1) USC Epigenome Center 7 2) USC/Norris Comprehensive Cancer Center 8 3) Division of Bioinformatics, Department of Preventive Medicine 9 4) Graduate Program in Genetic, Molecular and Cellular Biology 10 University of Southern California, Los Angeles, CA * Current address: Active Motif, Carlsbad, CA 11 12 # Contact info: 13 14 Benjamin P. Berman (bberman@usc.edu) 15 **USC** Epigenome Center 16 1450 Biggy St., #G511 17 Los Angeles, CA 90033 18 Ph: 323-442-7820

Δ	hei	tra	ct

2	Nucleosome organization and DNA methylation are two epigenetic mechanisms
3	that are important for proper control of mammalian transcription. Numerous lines of
4	evidence suggest an interaction between these two mechanisms, but the nature of this
5	interaction in vivo remains elusive. Whole-genome DNA methylation sequencing
6	studies have shown that human methylation levels are periodic at intervals of
7	approximately 190 bp, suggesting a genome-wide relationship between the two marks.
8	A recent report (Chodavarapu et al. 2010) attributed this to higher methylation levels of
9	DNA within nucleosomes. Here, we propose an alternate explanation for these
10	nucleosomal periodicities. By examining methylation patterns in published datasets, we
11	find that genome-wide methylation levels are highest within the linker regions that
12	occur between nucleosomes in multi-nucleosome arrays. This effect is most prominent
13	within long-range Partially Methylated Domains (PMDs) and the strongly positioned
14	nucleosomes that flank CTCF binding sites. The CTCF-flanking nucleosomes retain
15	positioning even in regions completely devoid of CpG dinucleotides, suggesting that
16	DNA methylation is not required for proper positioning. We propose that DNA
17	methylation is inhibited by histone proteins at CTCF and other unknown classes of
18	nucleosomes within PMDs.

Introduction

Packaging of DNA by nucleosomal proteins is an essential property of chromatin organization, and the precise positioning of individual nucleosomes at regulatory elements including promoters (Schones et al. 2008), enhancers (He et al. 2010), and insulators (Fu et al. 2008) is important for proper gene regulation (Iyer 2012). Methylation of DNA at CpG dinucleotides also plays an important role in the regulation of transcription in mammals, and recent work has shown dynamic methylation changes occur at these same regulatory elements (Gifford et al. 2013; Stadler et al. 2011; Wang et al. 2012; Xie et al. 2013). There is an intense interest in these two marks given that the genes controlling their deposition and removal are among the most commonly mutated in cancers (Dawson & Kouzarides 2012; You & Jones 2012).

Recent advances in DNA sequencing have facilitated the production of maps covering the entire genome at single nucleotide resolution for both nucleosome positioning (Schones et al. 2008) and DNA methylation (Lister et al. 2009), yet the relationship between the two is poorly understood. In plants, methylation between cytosines in the CHG context was correlated at intervals of 175 base pairs, strongly suggesting an association with nucleosome positioning (Cokus et al. 2008), but CHG methylation is not conserved in mammals. Comparing nucleosome positions genomewide in plants and human embryonic stem cells showed a modest (roughly 2%) increase in DNA methylation over the nucleosome core, along with a 10bp periodicity that suggested methylation occurred specifically at positions where the major groove faced away from histone proteins (Chodavarapu et al. 2010). More recently, *in vitro* nucleosome formation experiments showed that DNA methylation at the nucleosome core can promote the formation of a particular class of nucleosomes (Collings et al. 2013).

All of these earlier studies relied on MNase sequencing to define nucleosome positions *in vivo* and *in vitro*. Because MNase-seq and other "read enrichment" methods are known to introduce certain biases related to G/C content and other sequence composition (Benjamini & Speed 2012; Dohm et al. 2008; Harismendy et al. 2009), we

- developed a technique that does not depend on read enrichment to determine
- 2 nucleosome positions, but rather uses a methyltransferase footprinting method (Kelly et
- al. 2012). NOMe-seq is based on bisulfite sequencing, and is therefore internally
- 4 controlled for PCR and other steps that create skewed biases in read enrichment. We
- 5 used NOMe-seq to investigate well-positioned arrays of nucleosomes surrounding
- 6 CTCF binding sites, and discovered that DNA methylation was approximately two-fold
- 7 higher in linker regions between nucleosomes than it was within the nucleosomes
- 8 themselves (Kelly et al. 2012). This association with linker DNA was much stronger
- 9 than the association reported previously for nucleosomal DNA (Chodavarapu et al.
- 10 2010), prompting us to re-analyze existing data in an attempt to reconcile these two
- results. It is worth noting that the two seemingly opposite associations are not mutually
- exclusive; methylation could be highest within linkers for some genomic elements, and
- highest in nucleosomes for others.

Results

- We first performed the same analysis of (Chodavarapu et al. 2010), aligning HSF1
- 17 embryonic stem cell DNA methylation levels to all MNase fragments from a CD4+ T-
- cell library (Schones et al. 2008). This showed the same roughly 2% increase in
- methylation levels over the fragments, along with a clear 10-bp periodicity (Figure 1a).
- 20 Reasoning that a deproteinated ("naked") DNA control would be completely devoid of
- 21 in vivo nucleosome positioning information, we repeated the same analysis using a
- control library of naked HeLa DNA generated by the ENCODE project (Auerbach et al.
- 23 2009) (Figure 1a, pink lines). This data was generated by whole-genome sequencing of
- 24 completely deproteinated genomic DNA that was fragmented by sonication.
- 25 Methylation patterns aligned to these control fragments showed similar methylation
- patterns as the alignments to MNase based nucleosome fragments, suggesting a
- 27 potential technical effect. We examined G/C content and found that fragments of both
- 28 libraries were G/C rich, a factor known to introduce bias during the amplification
- 29 involved in next-generation sequencing (Benjamini & Speed 2012). Why this G/C

1	richness would cause higher methylation levels is not entirely understood, but it could
2	be caused by a concomitant enrichment of CpG dinucleotides. While the mechanism is
3	not understood, it is known that local CpG density is positively correlated with DNA
4	methylation level ((Edwards et al. 2010) and Supplemental Figure S1).
5	In an effort to identify nucleosome localization genome-wide without the potential
6	influence of G/C content skew associated with individual sequencing fragments, we
7	investigated the patterns of arrays of adjacent nucleosomes. It is clear from auto
8	alignment of the MNase data that multi-nucleosome arrays are present throughout the
9	genome (Figure 1b). We looked at methylation within an expanded region surrounding
10	nucleosomes in whole-genome bisulfite sequencing (WGBS) data for cell types
11	generated by different labs, including H1 (Lister et al. 2009) and HSF1 embryonic stem
12	cells (Chodavarapu et al. 2010), IMR90 fibroblasts (Lister et al. 2009), normal and
13	tumor colon tissue (Berman et al. 2012), and B-lymphocytes (Ball et al. 2009) (Figure
14	1c). Importantly, we included a dataset that was generated with a non-bisulfite
15	approach, Methylation Sensitive Restriction Enzyme (MSRE) sequencing, to rule out
16	any technical bisulfite effects. In all WGBS datasets, increased methylation was
17	observed over MNase fragments. In both HSF1 (Chodavarapu et al. 2010) and IMR90
18	(Lister et al. 2009), this pattern was similar to the pattern for the naked DNA control
19	(Figure 1c, right panel). When examining methylation levels outside the fragment itself,
20	patterns in the MNase data diverged from the naked DNA control. All libraries except
21	the most highly methylated hESC libraries showed increased methylation in inter-
22	nucleosome linker regions (Figure 1c, left panel), supporting the relationship we had
23	earlier observed in IMR90 nucleosomes adjacent to CTCF sites (Kelly et al. 2012). This
24	relationship was strongest for the MSRE library, indicating a generality across cell
25	types and methylation assays.
26	Next, we used the same analysis described above to investigate linker-specific
27	IMR90 methylation in different genomic contexts. We were interested to see if
28	methylated linkers were more prominent between nucleosomes positioned by CTCF

binding sites as found previously (Kelly et al. 2012), or within Partially Methylated

- 1 Domains (PMDs) which have more variable methylation levels than the rest of the
- 2 genome (Lister et al. 2009). Indeed, linkers within PMDs and near CTCF sites were
- 3 more strongly methylated than within non-PMDs (Figure 2a). CTCF regions showed the
- 4 most dramatic linker-specific methylation, perhaps because they are the most
- 5 consistently positioned class of nucleosomes in the genome. While the region
- 6 immediately overlapping MNase fragments had strongly biased sequence composition,
- 7 linker regions between nucleosomes had no sequence composition bias in any of the
- 8 genomic contexts (Figure 2b). To validate genome-wide linker methylation, we
- 9 identified consistent linker regions from IMR90 NOMe-seq nucleosome occupancy data
- 10 (Kelly et al. 2012) (Figure 2c). DNA within the linkers was consistently more
- methylated than the flanking nucleosomes, most prominently in CTCF regions and
- 12 PMDs. Interestingly, in both MNase and NOMe-seq analysis, the inter-nucleosome
- spacing was shorter in CTCF regions (185bp) than PMDs or the rest of the genome
- 14 (200bp). Genome-wide, we found that PMDs contained the bulk of all detectable
- nucleosomal periodicity (Figure 3).
- To demonstrate that increased methylation in linker DNA was not cell type
- 17 specific, we examined methylation around CTCF sites in several additional WGBS
- datasets as well as the non-bisulfite MSRE dataset described above. Indeed, all cell
- 19 types showed linker-specific methylation (Figure 4a), and almost identical global
- 20 patterns have been observed for dozens of other human tissues sequenced by WGBS in
- our lab (unpublished and data not shown). Interestingly, whereas CpGs within +/-
- 22 200bp of the CTCF binding site were completely unmethylated in most tissues, H1 and
- HSF1 embryonic stem cells (hESCs) showed increased methylation, possibly
- 24 attributable to ESC-specific 5-hydroxymethylation at CTCF sites (Yu et al. 2012).
- 25 MSRE could not accurately represent the methylation levels within this +/- 200bp
- region due to known limitations of the method to measure very low methylation (Ball et
- 27 al. 2009).
- The large number of CTCF binding sites in the genome provided an opportunity
- 29 to investigate the interplay between methylation and nucleosome positioning. There is

- 1 evidence suggesting that methylation can influence nucleosome formation (Collings et
- 2 al. 2013) and vice-versa (Ooi et al. 2007). It is impossible to determine with certainty
- 3 without additional experiments, but we reasoned that if DNA methylation were required
- 4 for nucleosome positioning, CpGs dinucleotides would be required around functional
- 5 CTCF sites. To investigate this bioinformatically, we extracted CTCF-adjacent
- 6 positions that contained zero CpGs in the reference human genome within a region of
- two full nucleosomes (+/-370bp). According to MNase occupancy and NOMe-seq
- 8 chromatin accessibility levels, the nucleosomes at these "zero CpG" regions were
- 9 positioned just as well as other CTCF-adjacent nucleosomes, strongly suggesting that
- 10 linker DNA methylation is not necessary for nucleosome positioning (Figure 4b-c).
- 11 Nevertheless, the "zero CpG" regions comprise only about 1-3% of CTCF-adjacent
- 12 nucleosomes, so we can not completely rule out some role for DNA methylation in
- establishing or reinforcing nucleosome positioning.

15

Discussion

- We have provided strong evidence for a pervasive methylation pattern occurring
- 17 at linker regions between arrays of positioned nucleosomes in the human genome. This
- observation has implications for methylome analysis, suggesting that methylation levels
- 19 may be used to deduce nucleosome positioning in some cases. Nucleosomes adjacent to
- 20 CTCF binding sites may account for a significant fraction of these nucleosomal arrays,
- 21 since it is estimated that approximately one million nucleosomes may be positioned
- adjacent to CTCF sites (around 55,000 CTCF sites in any given cell type (Wang et al.
- 23 2012), with about 20 nucleosomes positioned per site (Fu et al. 2008)). We additionally
- showed that methylation levels within linker regions are unlikely to play a causal role in
- 25 the positioning of CTCF-adjacent nucleosomes. This is parsimonious with the
- observation that strongly positioned nucleosomes are stacked against a barrier
- 27 introduced by ATP-dependent nucleosome remodeling (Zhang et al. 2011).
- 28 Inhibition of DNA methylation has been demonstrated for certain histone
- 29 modifications, including H3K4me1 (Ooi et al. 2007) and H2A.Z (Zilberman et al.

- 1 2008). Because CTCF-adjacent nucleosomes are marked by both of these modifications,
- 2 it is attractive to hypothesize that inhibition by these modifications does not extend into
- 3 the linker regions, leaving them open to DNA methyltransferase activity. We did
- 4 observe significant nucleosomal periodicity in regions outside of known CTCF sites
- 5 (data not shown), and we found that the bulk of this periodicity was within PMD
- 6 regions (Figure 3), which are depleted for active histone marks such as H3K4me1 and
- 7 H2A.Z. The higher level of nucleosomal periodicity detected within PMDs may be a
- 8 consequence the high methylation state maintained outside of PMDs (Raddatz et al.
- 9 2012). Further analysis is necessary to identify precise histone modification of
- 10 nucleosomes and methylation status in the same reference cell type.

Finally, based on our observations of methylation patterns within MNase and

12 naked DNA sequencing fragments, we also suggest that appropriate controls are

13 necessary for MNase-seq to rule out small biases introduced by next-generation

sequencing. G/C content and MNase-specific cleavage biases are known to be difficult

15 confounders of MNase-seq (Chung et al. 2010; Zhang et al. 2009), and we have

proposed NOMe-seq (Kelly et al. 2012) as a complementary strategy that can be used to

validate any results that might be affected by sequence-specific biases.

18

20

19

Methods

- 21 *CpG methylation datasets*: Percent methylation was taken from WGBS supplemental
- data files from Lister et al. (Lister et al. 2009) (IMR90, H1) and Berman et al. (Berman
- et al. 2012) (tumor colon and normal, GEO GSE32399). For B-lymphocyte MSRE
- dataset, supplemental data files from Ball et al. (Ball et al. 2009) contained the number
- of tag counts for each possible HspII site. Using the procedure described in the Ball et
- al. "methods" section, we transformed these counts to percent methylation using the
- following equation: $\mathbf{m} = 1 (0.1124 * \mathbf{c})$, where \mathbf{m} is the estimated percent methylation,
- and **c** is the raw tag counts.

28

1	<i>IMR90 NOMe seq data</i> : NOMe-seq data was taken from Kelly et al. (Kelly et al. 2012)
2	(GEO GSE40770). A beta-binomial Hidden Markov Model (HMM) (Molaro et al.
3	2011) was used to identify linker regions (manuscript in preparation).
4	
5	IMR90 MNase-seq (figure 4 only): IMR90 cells were cultured according to ATCC's
6	guidelines. Mononucleosomes were generated by digesting 1x10 ⁶ cells with 0.5, 1 and 5
7	Units of micrococcal nuclease (MNase; Worthington Biochemicals) for 15 minutes at
8	37 °C. The three MNase preparations were combined, and mononucleosome fragments
9	of ~150 bp were gel extracted and libraries were preparared from 30ng DNA using
10	Illumina single-end sequencing adapters as described in (Bernstein et al. 2006).
l 1	Sequencing was performed on an Illumina Genome Analyzer IIx using standard
12	Illumina reagents, producing 153,469,077 high quality 36bp sequence reads. Reads
13	were aligned using MAQ with a minimum mapping quality of 30, resulting in
14	111,705,730 uniquely alignable reads. All sequences and alignments are available at
15	GEO GSE21823.
16	
17	Nucleosome occupancy score (Figure 4 only): For genomic coordinate c and an
18	estimated mononucleosome size \mathbf{s} , the nucleosome occupancy score for a particular
19	position was determined by summing the number of MNase tags on the forward
20	genomic strand in the range \mathbf{c} -($\mathbf{s}/2$) and the number of tags on the reverse strand in the
21	range $c+(s/2)$. We estimated s to be 165 after examining a range of values (50bp-250bp)
22	within 1kb of all CTCF binding sites. After alignment to the genomic element of
23	interest, the raw nucleosome occupancy score was normalized for local tag density by
24	dividing by the total number of reads within 200bp. Plots were smoothed by taking a
25	moving average of normalized occupancy scores within a 20bp window.
26	

CTCF datasets: CTCF binding sites were taken from (Berman et al. 2012). For "CTCF

regions with 0 CpGs", we used only those genomic positions that contained no CpGs in

- 1 the reference human genome within a span of two nucleosomes on either side (+/-
- 2 370bp). This comprised about 1% of the full CTCF set.

1 **Author Contributions**

- 2 BPB and YL performed data analysis. TKK performed MNase-seq experiments and
- 3 helped interpret results. BPB conceived the study, supervised the work, and wrote the
- 4 manuscript.

5

6

Acknowledgements

- 7 We wish to thank Peter Jones for his suggestions and for fostering a supportive and
- 8 collaborative environment, and Huy Dinh and Fides Lay for helpful comments on the
- 9 manuscript. We are grateful to Charlie Nicolet, Selene Tyndale, and Helen Truong of
- 10 the Norris Molecular Genomics Core at the USC Epigenome Center for generating the
- sequencing data. Computation was performed at the USC High Performance Computing
- and Communications Center (http://www.usc.edu/hpcc/). This project described was
- supported in part by T32CA00932027 from the National Cancer Institute to TKK, and
- the generous support of the Kenneth T. and Eileen L. Norris Foundation to YL and
- BPB. It was also supported in part by award number P30CA014089 from the National
- 16 Cancer Institute. The content is solely the responsibility of the authors and does not
- 17 necessarily represent the official views of the National Cancer Institute or the National
- 18 Institutes of Health.

19

Fig	ure	Leg	ends

3 Figure 1: Methylation levels relative to MNase-seq fragments. (A) Including 4 an additional control to the analysis performed by Chodavarapu et al. 5 (Chodavarapu et al. 2010) shows that HSF1 methylation levels are increased 6 over the MNase fragments from the CD4+ T-cell dataset used in Chodavarapu 7 et al. (red line), but are also increased over fragments from a whole-genome sequencing library generated by sonication of deproteinated ("naked") genomic 8 9 DNA (pink line). The right panel shows elevated G/C content levels over these 10 same fragments. (B) Alignment of MNase cut sites relative to MNase fragments 11 reveals ordered arrays of nucleosomes, suggesting pervasive nucleosomal 12 arrays genome-wide. (C) Various WGBS methylation levels are aligned to 13 MNase (left) and Naked DNA (right) fragments, along with a methylation library 14 generated with non-bisulfite MSRE sequencing (see text). Elevated methylation

17

18

15

16

Figure 2: Increased methylation in linker regions within different genomic

levels are observed covering both MNase and Naked DNA fragments, but linker

- contexts. (A) IMR90 methylation patterns around MNase fragments were
- 20 plotted as in Figure 1, but stratified by genomic context. IMR90 Partially

regions are elevated only relative to MNase library.

- 21 Methylated Domains (PMDs) are from (Lister et al. 2009), while non-PMD
- 22 contains the remainder of the genome. See the methods section for a
- 23 description of CTCF binding sites. The left column shows methylation on a
- 24 consistent scale, while the middle column zooms into a scale relevant for each
- context. (B) Local CpG density aligned to the same MNase fragments. (C)
- 26 Linkers identified from IMR90 NOMe-seq (Kelly et al. 2012) are shown aligned
- to IMR90 chromatin accessibility (GCH, green line) and methylation (HCG,
- black line). H can include any A, C, or T nucleotide.

1	
2	Figure 3: Linker-specific methylation is higher within PMDs. (B)
3	Concordance between nearby CpGs. This was defined as the fraction of reads
4	that were methylated at a given CpG, plotted as a function of the genomic
5	distance from a reference methylated CpG (mCpG). If the target CpG had
6	multiple reference mCpGs within 2kb interval, it was counted separately for
7	each.
8	
9	Figure 4: DNA methylation occurs primarily at linker regions in
10	nucleosomal arrays flanking CTCF binding sites. (A) Methylation levels
11	around motifs bound by CTCF in HeLa cells (see methods). Association
12	between methylation and nucleosome positioning is verified in several WGBS
13	datasets and one non-bisulfite (MSRE) dataset. (B) Nucleosome occupancy is
14	shown around CTCF sites for IMR90 cells. The black line includes all CTCF-
15	adjacent regions from Figure 4a. The red line includes only positions that have
16	zero CpGs within +/-370 base pairs (a region the size of four full nucleosomes).
17	(C) Same analysis, but using NOMe-seq chromatin accessibility from IMR90
18	cells (Kelly et al. 2012).
19	
20	Supplemental Figure S1: Genome-wide correlation between local CpG
21	density and DNA methylation. (A) Data from IMR90 cells (Lister et al. 2009)
22	was extracted from all non-overlapping 100bp bins on chr17, and ranked by
23	CpG density. Groups of 100 bins were averaged to show CpG density, CpG
24	methylation, and tag density for H3K4me3 ChIP-seq. At CpGs without K4me3
25	mark, increasing local CpG density is correlated with DNA methylation level. (B)
26	The reason for this is unknown, but this is an agreement with an earlier study of
27	human breast and brain tissues (Edwards et al. 2010).

1	References

7

8

9

10

11 12

13

14

15

16

17

18

19

20

21

22

23

24

25

26

27

28

29

30

31

- 3 Auerbach RK, Euskirchen G, Rozowsky J, Lamarre-Vincent N, Mogtaderi Z, 4 Lefrançois P, Struhl K, Gerstein M, and Snyder M. 2009. Mapping accessible 5 chromatin regions using Sono-Seq. Proceedings of the National Academy of 6 Sciences of the United States of America 106:14926-14931.
 - Ball MP, Li JB, Gao Y, Lee J-H, LeProust EM, Park I-H, Xie B, Daley GQ, and Church GM. 2009. Targeted and genome-scale strategies reveal gene-body methylation signatures in human cells. *Nature biotechnology* 27:361-368.
 - Benjamini Y, and Speed TP. 2012. Summarizing and correcting the GC content bias in high-throughput sequencing. Nucleic acids research 40:e72.
 - Berman BP, Weisenberger DJ, Aman JF, Hinoue T, Ramjan Z, Liu Y, Noushmehr H, Lange CPE, van Dijk CM, Tollenaar RaEM et al. . 2012. Regions of focal DNA hypermethylation and long-range hypomethylation in colorectal cancer coincide with nuclear lamina-associated domains. *Nature genetics* 44:40-46.
 - Bernstein BE, Mikkelsen TS, Xie X, Kamal M, Huebert DJ, Cuff J, Fry B, Meissner A, Wernig M, Plath K et al. . 2006. A bivalent chromatin structure marks key developmental genes in embryonic stem cells. *Cell* 125:315-326.
 - Chodavarapu RK, Feng S, Bernatavichute YV, Chen P-Y, Stroud H, Yu Y, Hetzel Ja, Kuo F, Kim J, Cokus SJ et al. . 2010. Relationship between nucleosome positioning and DNA methylation. *Nature* 466:388-392.
 - Chung H-R, Dunkel I, Heise F, Linke C, Krobitsch S, Ehrenhofer-Murray AE, Sperling SR, and Vingron M. 2010. The effect of micrococcal nuclease digestion on nucleosome positioning data. *PloS one* 5:e15754.
 - Cokus SJ, Feng S, Zhang X, Chen Z, Merriman B, Haudenschild CD, Pradhan S, Nelson SF, Pellegrini M, and Jacobsen SE. 2008. Shotgun bisulphite sequencing of the Arabidopsis genome reveals DNA methylation patterning. *Nature* 452:215-219.
 - Collings CK, Waddell PJ, and Anderson JN. 2013. Effects of DNA methylation on nucleosome stability. *Nucleic acids research*:1-14.
 - Dawson Ma, and Kouzarides T. 2012. Cancer epigenetics: from mechanism to therapy. *Cell* 150:12-27.
- 33 Dohm JC, Lottaz C, Borodina T, and Himmelbauer H. 2008. Substantial biases in ultra-34 short read data sets from high-throughput DNA sequencing. *Nucleic acids* 35 research 36:e105.
- 36 Edwards JR, O'Donnell AH, Rollins Ra, Peckham HE, Lee C, Milekic MH, Chanrion B, 37 Fu Y, Su T, Hibshoosh H et al. . 2010. Chromatin and sequence features that define the fine and gross structure of genomic methylation patterns. Genome 38 39 research 20:972-980.
- 40 Fu Y, Sinha M, Peterson CL, and Weng Z. 2008. The insulator binding protein CTCF 41 positions 20 nucleosomes around its binding sites across the human genome. 42
- PLoS genetics 4:e1000138.

10

11

14

15

16

17

18

19

20

21

22

23

24

25

26

27

28

32

33

- Gifford CA, Ziller MJ, Gu H, Trapnell C, Donaghey J, Tsankov A, Shalek AK, Kelley DR, Shishkin AA, Issner R et al. . 2013. Transcriptional and Epigenetic Dynamics during Specification of Human Embryonic Stem Cells. *Cell* 153:1149-1163.
- Harismendy O, Ng PC, Strausberg RL, Wang X, Stockwell TB, Beeson KY, Schork NJ,
 Murray SS, Topol EJ, Levy S et al. . 2009. Evaluation of next generation
 sequencing platforms for population targeted sequencing studies. *Genome* biology 10:R32.
 - He HH, Meyer Ca, Shin H, Bailey ST, Wei G, Wang Q, Zhang Y, Xu K, Ni M, Lupien M et al. . 2010. Nucleosome dynamics define transcriptional enhancers. *Nature genetics* 42:343-347.
- Iyer VR. 2012. Nucleosome positioning: bringing order to the eukaryotic genome.
 Trends in cell biology 22:250-256.
 - Kelly TK, Liu Y, Lay FD, Liang G, Berman BP, and Jones Pa. 2012. Genome-wide mapping of nucleosome positioning and DNA methylation within individual DNA molecules. *Genome research* 22:2497-2506.
 - Lister R, Pelizzola M, Dowen RH, Hawkins RD, Hon G, Tonti-Filippini J, Nery JR, Lee L, Ye Z, Ngo Q-m et al. . 2009. Human DNA methylomes at base resolution show widespread epigenomic differences. *Nature* 462:315-322.
 - Molaro A, Hodges E, Fang F, Song Q, McCombie WR, Hannon GJ, and Smith AD. 2011. Sperm methylation profiles reveal features of epigenetic inheritance and evolution in primates. *Cell* 146:1029-1041.
 - Ooi SKT, Qiu C, Bernstein E, Li K, Jia D, Yang Z, Erdjument-Bromage H, Tempst P, Lin S-P, Allis CD et al. . 2007. DNMT3L connects unmethylated lysine 4 of histone H3 to de novo methylation of DNA. *Nature* 448:714-717.
 - Raddatz G, Gao Q, Bender S, Jaenisch R, and Lyko F. 2012. Dnmt3a protects active chromosome domains against cancer-associated hypomethylation. *PLoS genetics* 8:e1003146.
- Schones DE, Cui K, Cuddapah S, Roh T-Y, Barski A, Wang Z, Wei G, and Zhao K.
 2008. Dynamic regulation of nucleosome positioning in the human genome. *Cell* 132:887-898.
 - Stadler MB, Murr R, Burger L, Ivanek R, Lienert F, Schöler A, van Nimwegen E, Wirbelauer C, Oakeley EJ, Gaidatzis D et al. . 2011. DNA-binding factors shape the mouse methylome at distal regulatory regions. *Nature* 480:490-495.
- Wang H, Maurano MT, Qu H, Varley KE, Gertz J, Pauli F, Lee K, Canfield T, Weaver
 M, Sandstrom R et al. . 2012. Widespread plasticity in CTCF occupancy linked
 to DNA methylation. *Genome research* 22:1680-1688.
- Xie W, Schultz MD, Lister R, Hou Z, Rajagopal N, Ray P, Whitaker JW, Tian S,
 Hawkins RD, Leung D et al. . 2013. Epigenomic Analysis of Multilineage
 Differentiation of Human Embryonic Stem Cells. *Cell* 153:1134-1148.
- 41 You JS, and Jones Pa. 2012. Cancer genetics and epigenetics: two sides of the same coin? *Cancer cell* 22:9-20.

1	Yu M, Hon GC, Szulwach KE, Song C-X, Jin P, Ren B, and He C. 2012. Tet-assisted
2	bisulfite sequencing of 5-hydroxymethylcytosine. <i>Nature protocols</i> 7:2159-
3	2170.
4	Zhang Y, Moqtaderi Z, Rattner BP, Euskirchen G, Snyder M, Kadonaga JT, Liu XS,
5	and Struhl K. 2009. Intrinsic histone-DNA interactions are not the major
6	determinant of nucleosome positions in vivo. Nature structural & molecular
7	biology 16:847-852.
8	Zhang Z, Wippo CJ, Wal M, Ward E, Korber P, and Pugh BF. 2011. A packing
9	mechanism for nucleosome organization reconstituted across a eukaryotic
10	genome. Science (New York, NY) 332:977-980.
l 1	Zilberman D, Coleman-Derr D, Ballinger T, and Henikoff S. 2008. Histone H2A.Z and
12	DNA methylation are mutually antagonistic chromatin marks. <i>Nature</i> 456:125-
13	129.
14	

FIG 1

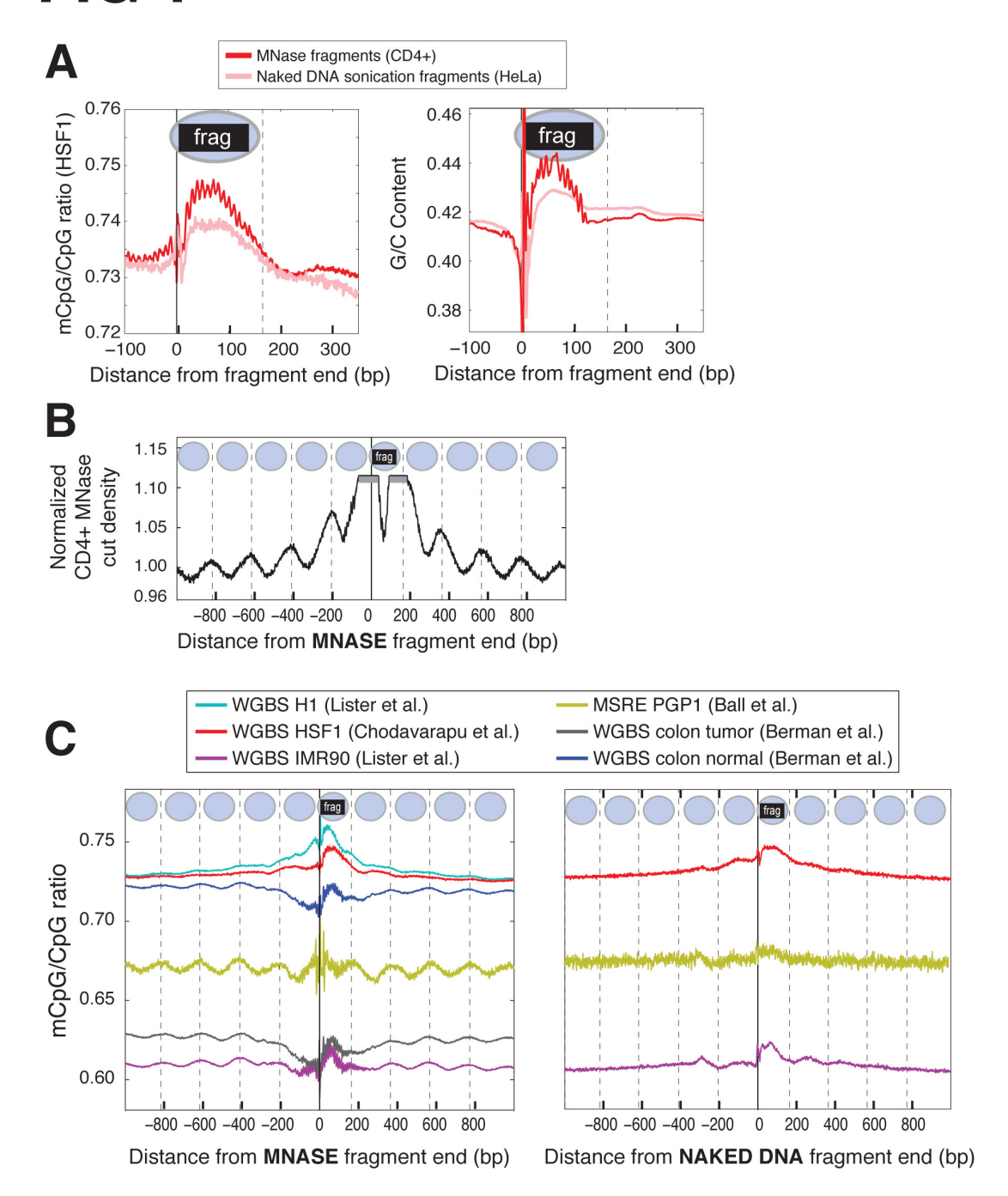


Figure 1: Methylation levels relative to MNase-seq fragments. (A) Including an additional control to the analysis performed by Chodavarapu et al. (Chodavarapu et al. 2010) shows that HSF1 methylation levels are increased over the MNase fragments from the CD4+ T-cell dataset used in Chodavarapu et al. (red line), but are also increased over fragments from a whole-genome sequencing library generated by sonication of deproteinated ("naked") genomic DNA (pink line). The right panel shows elevated G/C content levels over these same fragments. (B) Alignment of MNase cut sites relative to MNase fragments reveals ordered arrays of nucleosomes, suggesting pervasive nucleosomal arrays genome-wide. (C) Various WGBS methylation levels are aligned to MNase (left) and Naked DNA (right) fragments, along with a methylation library generated with non-bisulfite MSRE sequencing (see text). Elevated methylation levels are observed covering both MNase and Naked DNA fragments, but linker regions are elevated only relative to MNase library.

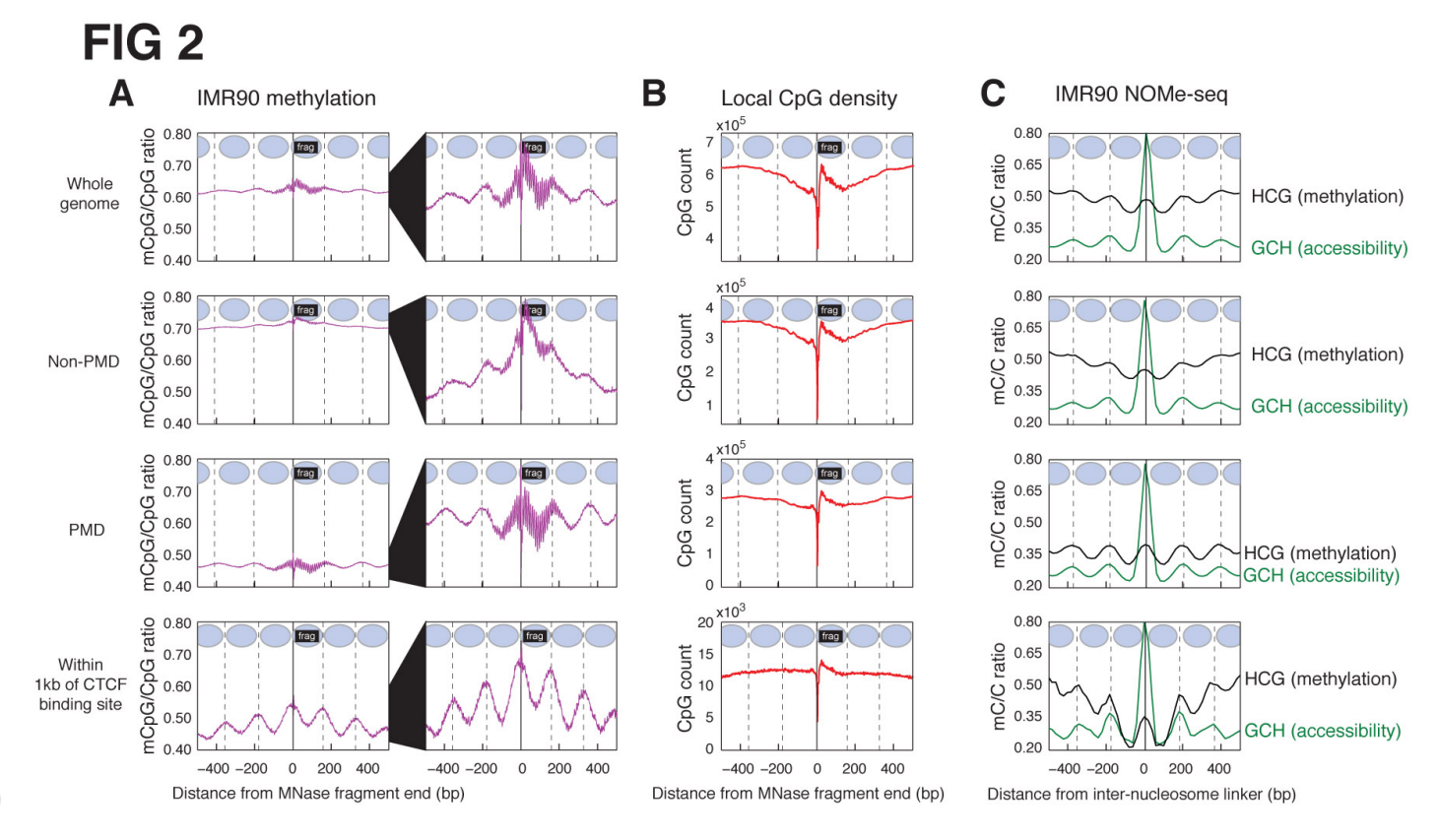


Figure 2: Increased methylation in linker regions within different genomic contexts. (A) IMR90 methylation patterns around MNase fragments were plotted as in Figure 1, but stratified by genomic context. IMR90 Partially Methylated Domains (PMDs) are from (Lister et al. 2009), while non-PMD contains the remainder of the genome. See the methods section for a description of CTCF binding sites. The left column shows methylation on a consistent scale, while the middle column zooms into a scale relevant for each context. (B) Local CpG density aligned to the same MNase fragments. (C) Linkers identified from IMR90 NOMe-seq (Kelly et al. 2012) are shown aligned to IMR90 chromatin accessibility (GCH, green line) and methylation (HCG, black line). H can include any A, C, or T nucleotide.

FIG 3

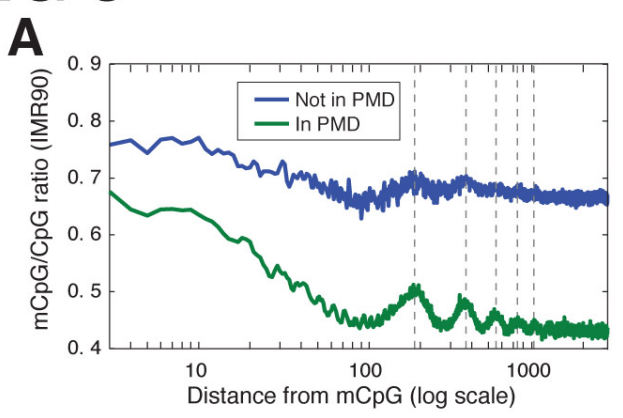
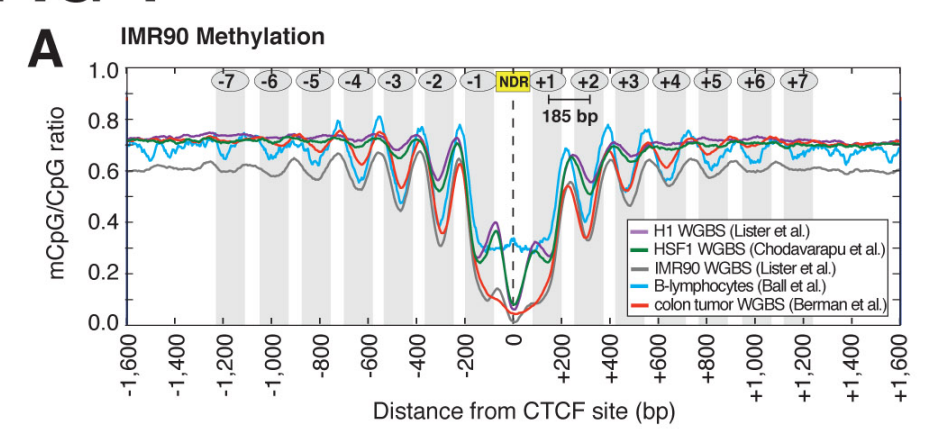
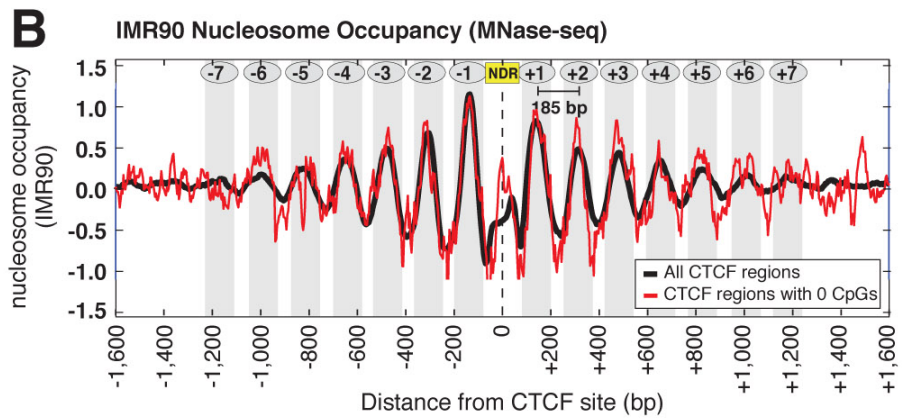


Figure 3: Linker-specific methylation is higher within PMDs. (B) Concordance between nearby CpGs. This was defined as the fraction of reads that were methylated at a given CpG, plotted as a function of the genomic distance from a reference methylated CpG (mCpG). If the target CpG had multiple reference mCpGs within 2kb interval, it was counted separately for each.

FIG 4





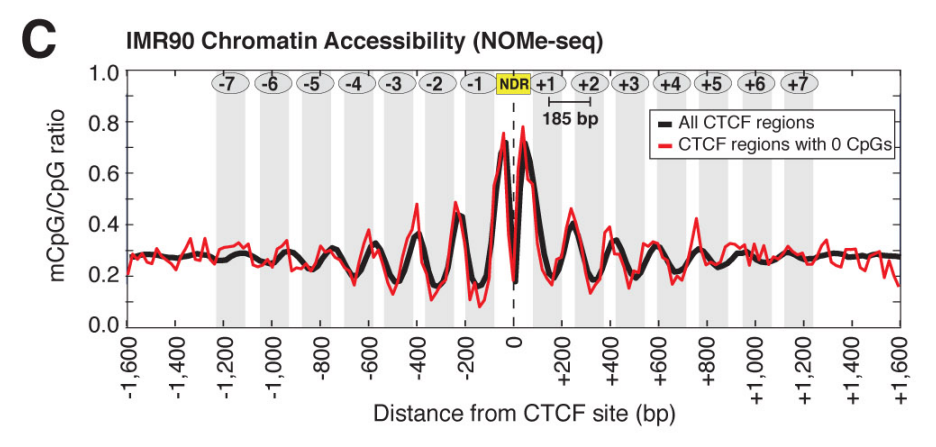
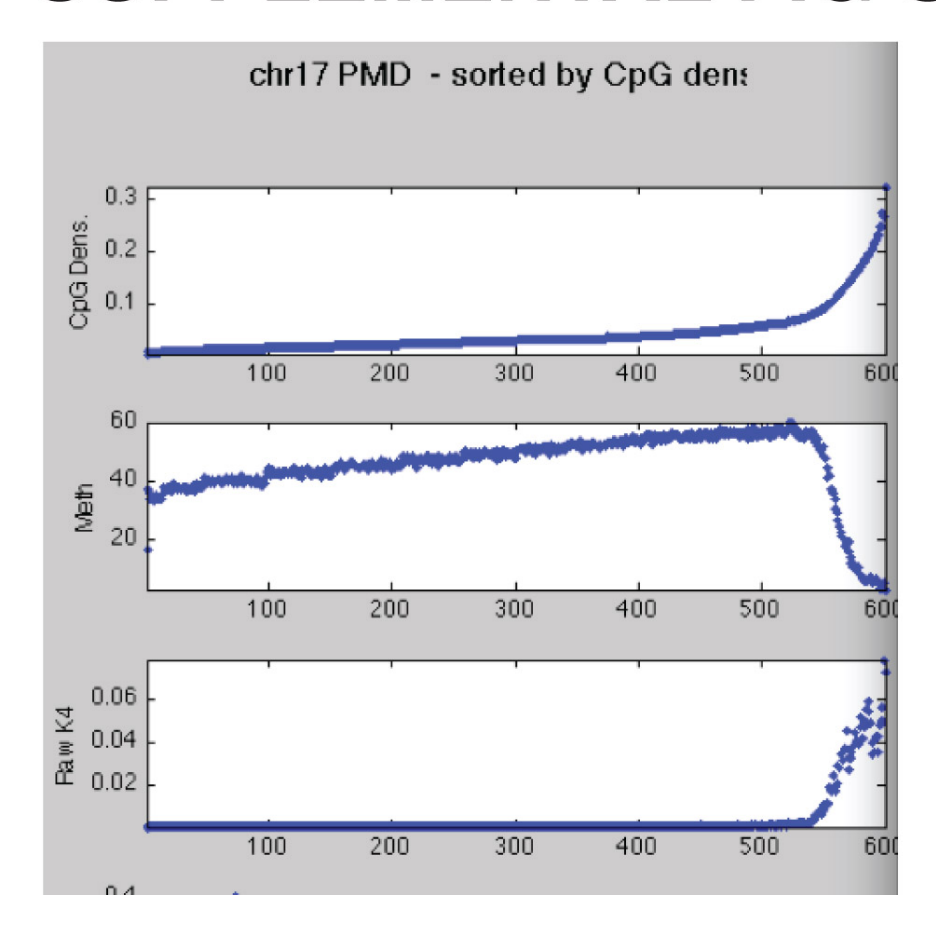


Figure 4: DNA methylation occurs primarily at linker regions in nucleosomal arrays flanking CTCF binding sites. (A) Methylation levels around motifs bound by CTCF in HeLa cells (see methods). Association between methylation and nucleosome positioning is verified in several WGBS datasets and one non-bisulfite (MSRE) dataset. (B) Nucleosome occupancy is shown around CTCF sites for IMR90 cells. The black line includes all CTCF-adjacent regions from Figure 4a. The red line includes only positions that have zero CpGs within +/-370 base pairs (a region the size of four full nucleosomes). (C) Same analysis, but using NOMe-seq chromatin accessibility from IMR90 cells (Kelly et al. 2012).

SUPPLEMENTAL FIG S1



Supplemental Figure S1: Genome-wide correlation between local CpG density and DNA methylation. (A) Data from IMR90 cells (Lister et al. 2009) was extracted from all non-overlapping 100bp bins on chr17, and ranked by CpG density. Groups of 100 bins were averaged to show CpG density, CpG methylation, and tag density for H3K4me3 ChIP-seq. At CpGs without K4me3 mark, increasing local CpG density is correlated with DNA methylation level. (B) The reason for this is unknown, but this is an agreement with an earlier study of human breast and brain tissues (Edwards et al. 2010).